Synchronizing Rock Clocks of Earth History

K. F. Kuiper, *et al.*
Science **320**, 500 (2008);
DOI: 10.1126/science.1154339

Synchronizing Rock Clocks of Earth History

K. F. Kuiper,[1,2] A. Deino,[3] F. J. Hilgen,[1] W. Krijgsman,[1] P. R. Renne,[3,4] J. R. Wijbrans[2]

Calibration of the geological time scale is achieved by independent radioisotopic and astronomical dating, but these techniques yield discrepancies of ~1.0% or more, limiting our ability to reconstruct Earth history. To overcome this fundamental setback, we compared astronomical and $^{40}Ar/^{39}Ar$ ages of tephras in marine deposits in Morocco to calibrate the age of Fish Canyon sanidine, the most widely used standard in $^{40}Ar/^{39}Ar$ geochronology. This calibration results in a more precise older age of 28.201 ± 0.046 million years ago (Ma) and reduces the $^{40}Ar/^{39}Ar$ method's absolute uncertainty from ~2.5 to 0.25%. In addition, this calibration provides tight constraints for the astronomical tuning of pre-Neogene successions, resulting in a mutually consistent age of ~65.95 Ma for the Cretaceous/Tertiary boundary.

Accurate and precise measurement of geological time is a prerequisite for understanding Earth's history. Numerical calibration of the geological time scale (GTS) [for example, GTS2004 (*1*)] is currently based on two independent techniques: astronomical tuning of cyclic sedimentary sequences, which provides a very accurate and high-resolution age model for the youngest Neogene part of the time scale, and radioisotopic dating for older time intervals. However, the various techniques often yield statistically different ages when applied to the same stratigraphic horizons (*2, 3*).

The radioisotopic dating technique most widely applicable to the late Cenozoic is the $^{40}Ar/^{39}Ar$

[1]Faculty of Geosciences, Department of Earth Sciences, Utrecht University, Budapestlaan 4, 3584 CD Utrecht, Netherlands. [2]Faculty of Earth and Life Sciences, Institute of Earth Sciences, Vrije Universiteit Amsterdam, De Boelelaan 1085, 1081 HV Amsterdam, Netherlands. [3]Berkeley Geochronology Center, 2455 Ridge Road, Berkeley, CA 94709, USA. [4]Department of Earth and Planetary Science, University of California, Berkeley, CA 94720, USA.

method. With careful attention to experimental design, it is possible to achieve analytical precision of 0.2% or better; however, the absolute accuracy of the technique is limited to ~2.5% (*4, 5*), mainly because of uncertainties in the ages of standards and radioactive decay rates (*6*).

Several attempts have been made to improve the technique's accuracy by calibrating the $^{40}Ar/^{39}Ar$ dating method to the astronomical method. However, these attempts were limited by uncertainties in identifying the location of magnetostratigraphic boundaries and their correlation to the astronomical polarity time scale (*7*), assumptions regarding constancy of sedimentation rates (*7*), complications associated with the use of geochronometers such as biotite (recoil, open-system alteration) and plagioclase (excess argon) (*8*), problems associated with multigrain sanidine experiments (masking complexities in age distributions) (*3*), or uncertainties in astronomical time control (*3, 9*).

We avoid these drawbacks by applying the single-crystal $^{40}Ar/^{39}Ar$ dating method to sanidine phenocrysts extracted from numerous silicic tephra layers intercalated in an astronomically tuned open marine succession from the Messinian Melilla Basin in Morocco. This basinal succession grades laterally into a marginal carbonate complex; the coarse-grained tephra are derived from the nearby Gourougou volcanic complex (*10, 11*). The astronomical tuning of the basinal precession–related marl-diatomite cycles is accomplished indirectly, because the sedimentary cycles lack the expression of characteristic details related to precession amplitude and precession-obliquity interference that are common in Mediterranean sapropel sequences (*12*). Selected planktonic foraminiferal bioevents known to be synchronous throughout the Mediterranean have been identified in the Melilla sections and are correlated to well-tuned Mediterranean reference sections (Fig. 1) (*11*) that form the core of the standard Neogene time scale (*12, 13*). The number of sedimentary cycles at Melilla between these biostratigraphic markers is consistent with the number found in these reference sections (*11, 12*). This indirect approach allows astronomical dating of each tephra layer (Fig. 1).

Uncertainties in the astronomical ages of the radioisotopically dated tephra horizons are contingent on (i) the applied astronomical solutions, including values for tidal dissipation and dynamical ellipticity; (ii) errors in interpolation resulting from the assumption of a constant sedimentation rate between two astronomically tuned calibration points [in this case, cycles are precession tuned and errors are therefore much less than 21 thousand years (ky)]; and (iii) the lag between the orbital forcing and sedimentary expression (we assume that the lag is zero). No exact error can be calculated, but taking these uncertainties into account and provided that the tuning and correlation itself is correct, we estimate that the uncertainty in the astronomical ages for the volcanic ash layers is ±10 ky.

Table 1. Recalculated ages of K-T boundary and early Paleocene geomagnetic polarity-reversal boundaries, in Ma. The $^{40}Ar/^{39}Ar$ ages of (*36–38*) are recalculated relative to the astronomically calibrated age of FCs (28.201 ± 0.046 Ma). An age of 28.02 Ma for FCs (*4*) is adopted in GTS2004. Reversal ages in GTS2004 are based on age calibration by spline fit of selected calibration points, including the K-T boundary with an age of 65.5 Ma. Recalculated radioisotopic ages are given with full error estimate. Details on the revised astronomical tuning are given in Fig. 4. The astronomical ages for the reversal boundaries and K-T boundary are calculated by counting the number of precession cycles from the nearest 100-ky eccentricity maximum/minimum. The age is then calculated by adding or subtracting this number multiplied with the 21-ky precession period to or from the age of the nearest eccentricity maximum or minimum. The astronomical error includes, under the assumption of a correct correlation to the 100-ky eccentricity maximum or minimum, the uncertainty in the 405-ky eccentricity cycle in astronomical solution (±40 ky) [figure 25 in (*35*)] and an additional error of ±15 ky for the uncertainty in the exact position of reversal boundaries. Chron, time interval between polarity reversals of Earth's magnetic field.

Chron / Boundary	GTS2004 (*1*)	Westerhold et al. (*39*) Option 1	Westerhold et al. (*39*) Option 2	Dinarès-Turell et al. (*33*)	Swisher et al. (*36, 37*)	Izett et al. (*38*)	Revised tuning (this study)‖
Reversal C28n (o)	64.128	64.028 ± 0.013	64.385 ± 0.013	64.460	64.6		64.698 ± 0.055 (64.663)
Reversal C29n (y)	64.432	64.205 ± 0.014	64.572 ± 0.016	64.670	64.9		64.884 ± 0.055 (64.835)
C29n (o)	65.118	64.912 ± 0.015	65.282 ± 0.016	65.549	65.4		65.724 ± 0.055 (65.702)
K-T	65.50 ± 0.30	65.280 ± 0.010	65.680 ± 0.010	65.777	65.81 ± 0.14* 65.84 ± 0.12† 65.99 ± 0.12‡ 65.84 ± 0.16§	65.98 ± 0.10§	65.957 ± 0.040 (65.940)

*Melt rock of Chicxulub crater. †Sanidine of Z coal. ‡Sanidine of IrZ coal. §Haïtian tektites. ‖Bracketed ages tuned to Va03_R7 (*44*).
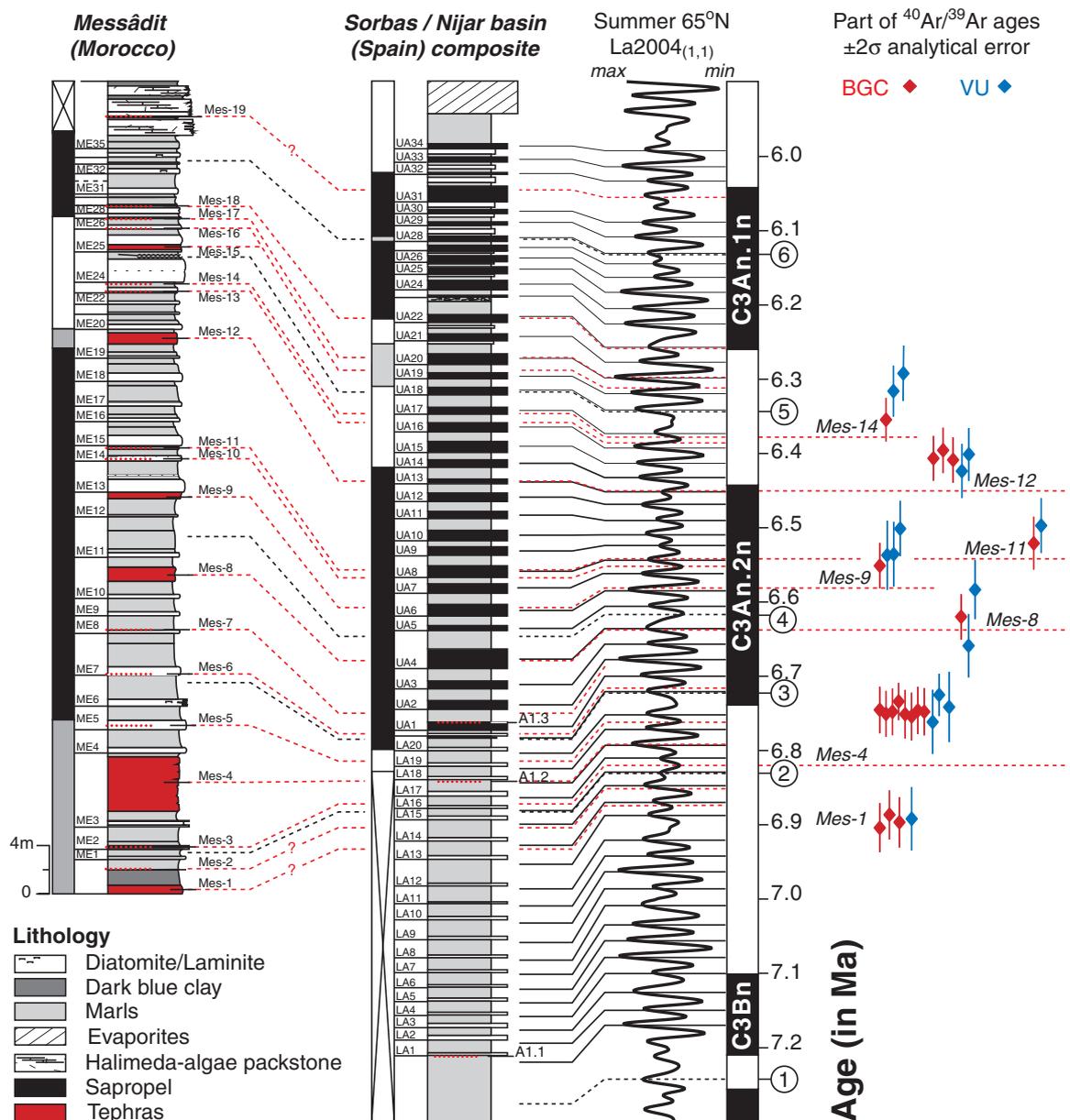
The ^{40}Ar/^{39}Ar dating of the Melilla tephra was performed in parallel at the Berkeley Geochronology Center (BGC) and the Vrije Universiteit Amsterdam (VU) (14). In general, ^{40}Ar/^{39}Ar ages measured in both laboratories are equivalent within 2σ analytical error (table S1), thus confirming a lack of significant interlaboratory bias at this level of confidence. These results can be converted to an astronomically calibrated age for Fish Canyon sanidine (FCs) by treating the Melilla sanidines as astronomically dated standards and FCs as the unknown (Fig. 2). After incorporating all known sources of error [analytical errors, uncertainty in the astronomical age, and a decay constant of $5.543 \pm 0.020) \times 10^{-10}$ year^{-1} (15)], the intercomparison yielded an age of 28.198 ± 0.044 million years ago (Ma). This approach involves the ^{40}K total decay constant, but is insensitive

to the value used or its uncertainty. A compilation of the underlying activity data and data updated with new values for other constants led Min *et al.* (5) to determine a value of $(5.463 \pm 0.214) \times 10^{-10}$ year^{-1} and showed the conventionally accepted error to be overly optimistic by an order of magnitude. Nonetheless, from this substantially less accurate (but more realistic) value we calculate an indistinguishable age (with negligibly increased uncertainty) of 28.201 ± 0.046 Ma for FCs. We propose that this result should be the age and uncertainty for FCs, rather than the widely used age of 28.02 ± 0.56 Ma (4). Our age is 0.65% older than the previous one, although given the larger uncertainty of the earlier value the two ages are statistically indistinguishable.

Comparison of our result with the U/Pb zircon age for the Fish Canyon Tuff is meaningless be-

cause of its complex crystallization history, lengthy residence time of zircon, and/or age bias due to Pb loss [for example, see (16–18)]. Comparison of conventional ^{40}Ar/^{39}Ar and U/Pb ages for diverse rock types over more than 3 billion years of geological time demonstrates a systematic offset, in which the U/Pb ages are older by 0 to 1% than the ^{40}Ar/^{39}Ar ages for the same rocks (19), although scatter in the offset suggests that some of the differences may result from interlaboratory biases or geological complexities. Mundil *et al.* (20) presented U/Pb (zircon) and ^{40}Ar/^{39}Ar ages for a suite of volcanic rocks between 130 Ma and 2.1 Ga; these results are likely free of detectable bias due to geological complexities (for example, magma residence time of the zircons, differential closure temperatures, or excess ^{40}Ar) or interlaboratory

Fig. 1. Astronomical calibration of Messinian Messâdit section in the Melilla-Nador Basin and ^{40}Ar/^{39}Ar ages of intercalated tephra. The cycles are tuned to the La2004$_{(1,1)}$ solution (35). The main biostratigraphic marker events registered within the studied sections and used for high-resolution correlations are (1) *Globorotalia miotumida* group first regular occurrence (FRO), (2) *G. nicolae* first common occurrence (FCO), (3) *G. nicolae* last occurrence (LO), (4) *G. obesa* FCO, (5) *Neogloboquadrina acostaensis* sinistral/dextral coiling change, and (6) *N. acostaensis* first sinistral influx (11, 12, 43). The phase relation of the sedimentary cycles to orbital parameters is determined using the exact position of bioevents and characteristic planktonic foraminiferal faunal changes associated with the sedimentary cyclicity in the pre-evaporite Messinian Sorbas basin (43). Homogeneous marls in the Moroccan sections correspond to sapropels in Sorbas and other Mediterranean sections (11). Astronomical ages for the tephras are derived by linear interpolation between two astronomically tuned points (that is, three-quarters of the height from the base of the homogeneous interval in each cycle is correlated to the insolation maximum). Weighted mean ^{40}Ar/^{39}Ar ages of tephra intercalated in the Messâdit section and analyzed in BGC and VU are shown, calculated relative to an age of 28.02 Ma for FCs (4) (table S1). The 2σ error bars include only analytical uncertainties of samples and standards.

errors, and yielded an age of 28.28 ± 0.06 Ma for FCs [21]. Thus, our astronomically tuned FCs age of 28.201 Ma is consistent at the 95% confidence level with normalization of the ^{40}Ar/^{39}Ar to the U/Pb system.

Further confirmation of consistency between the ^{40}Ar/^{39}Ar and U/Pb systems based on the proposed revised ^{40}Ar/^{39}Ar age of FCs comes from comparison of U/Pb and ^{40}Ar/^{39}Ar ages of chondritic meteorites, such as Acapulco [22] and Allende. A ~0.8 to 1% bias between the most accurate ^{40}Ar/^{39}Ar [23, 24] and U/Pb [25, 26] ages has classically been interpreted as evidence

for slow cooling after partial melting at 4555.1 ± 1.3 Ma (Acapulco) and formation at 4566.6 ± 1.7 Ma (Allende), as determined by U/Pb dating. With the revised age for the FCs, the K/Ar and U/Pb systems approach concordancy and instead suggest that the parent body of these meteorites cooled rapidly after formation, as suggested by (U+Th)/He [27] and I/Xe [28, 29] studies.
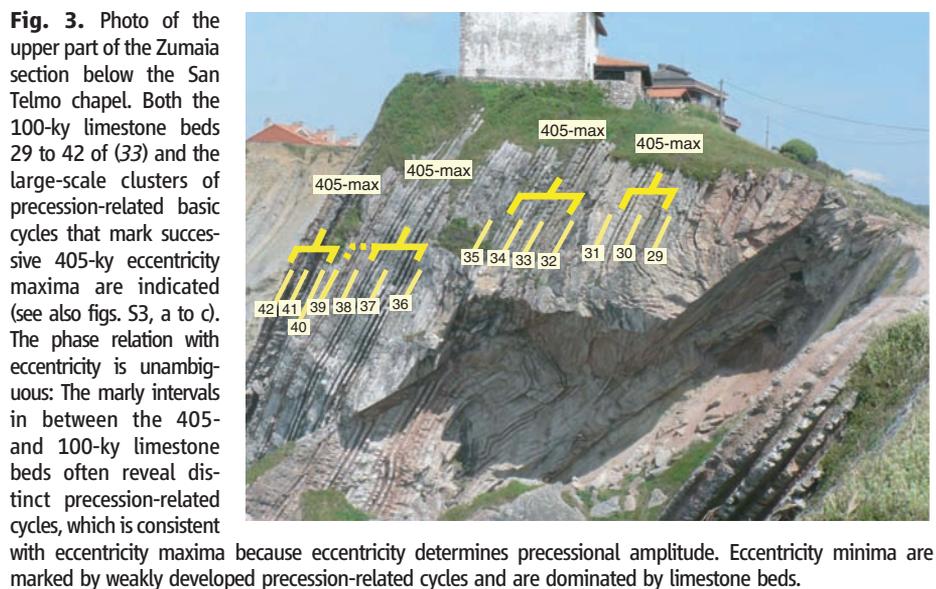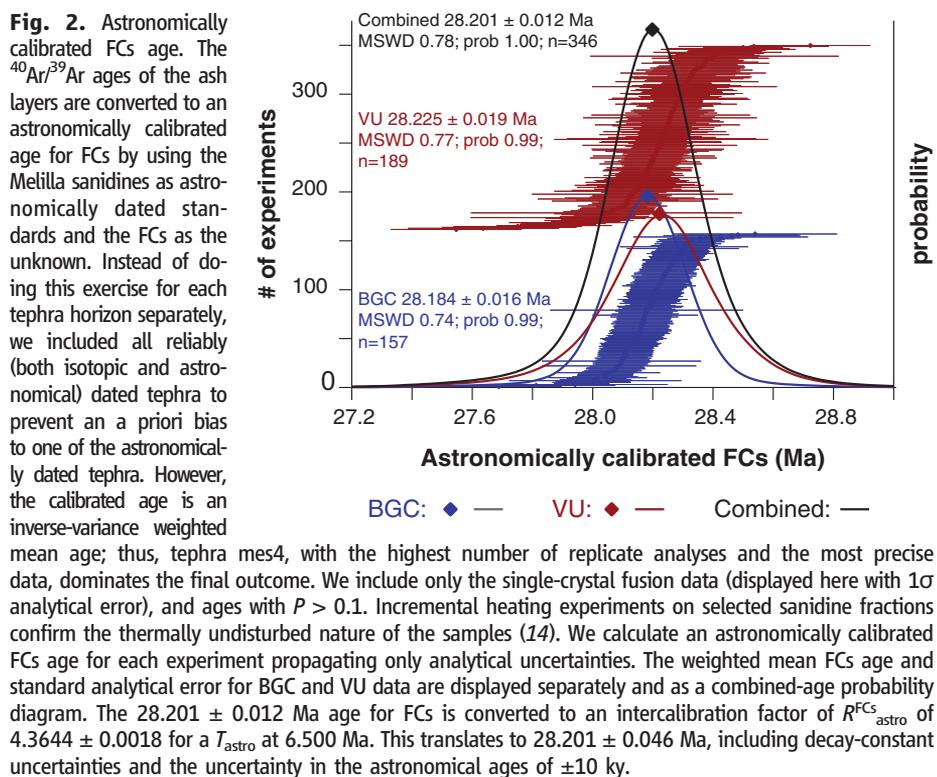
The astronomically calibrated FCs age thus eliminates the documented offset of the conventionally calibrated ^{40}Ar/^{39}Ar and U/Pb dating systems in many volcanic rocks. It also has implications for ages of geomagnetic polarity reversals over the past

3 million years (My). Numerous studies in the past two decades have demonstrated apparent consistency between the ^{40}Ar/^{39}Ar method and the astronomical dating approach in both sedimentary and volcanic settings, starting from a younger age for FCs or other standards (table S3). This implies that the new FCs age is not consistent with many of these results. For example, recalculating some ^{40}Ar/^{39}Ar dates for the Matuyama-Bruhnes reversal relative to our age for FCs yields radioisotopic ages older than the astronomical age [table S3 and references in [14]]. However, the most recent and comprehensive ^{40}Ar/^{39}Ar data [30], which suggested that the transition may have been diachronous, are in agreement with our intercalibration.

An important application of the astronomically calibrated ^{40}Ar/^{39}Ar method is to provide constraints for the astronomical tuning of pre-Neogene sequences. The prime, first-order target for tuning these older sequences is the 405-ky earth-orbital eccentricity cycle [31, 32]. Our method reduces the absolute uncertainty from ~2.5% (or ~1600 ky at 65 Ma) to potentially <0.25% (or <165 ky at 65 Ma), because the uncertainties in absolute amounts of radiogenic ^{40}Ar and ^{40}K in the primary standard and the branching ratio of the ^{40}K decay constant are circumvented using the astronomical age of the Melilla sanidines as the basis for calculating the ^{40}Ar/^{39}Ar age. The use of equation 5 of [4] enables calculation of the age of an unknown based on an age for the standard determined by means other than the K-Ar system, and requires only knowledge of the total ^{40}K decay constant (that is, not the branching ratio). [Full equations are provided in [14].]

We demonstrate the improved age resolution by examining the GTS2004 age of 65.5 Ma for the Cretaceous/Tertiary (K-T) boundary, which marks one of the most important biotic crises in Earth history. The K-T boundary section at Zumaia, Spain, which magnetostratigraphically covers the interval from the younger part of polarity interval C29r well into C26r, has been astronomically tuned and the boundary has been assigned an age of 65.777 Ma [33]. The astronomical age of [33] is uncertain for two reasons: (i) the use of the potentially unstable very-long-period 2.4-My eccentricity cycle as the starting point for the tuning; and (ii) the matching of basic marl/limestone cycle packages [the E-cycles of [33]] to successive 100-ky eccentricity minima in the target curve, which is less certain (and stable) than the 405-ky eccentricity minima (fig. S2).

According to [33], the 405-ky cycle is not expressed, or only very weakly present at Zumaia. Nevertheless, this cycle can be identified on photographs, in the field, and in the lithologic log of Zumaia of [33] through differences in the thickness and expression of marls intercalated between 100-ky limestone beds (Fig. 3 and fig. S3). Details of the cycle pattern confirm the phase relations between the sedimentary cycles and eccentricity as inferred by [33]. Small-scale precession-related cycles are less well developed in the limestone beds of eccentricity-related cycles, indicating that these beds indeed correspond to eccentricity minima be-

Fig. 2. Astronomically calibrated FCs age. The ^{40}Ar/^{39}Ar ages of the ash layers are converted to an astronomically calibrated age for FCs by using the Melilla sanidines as astronomically dated standards and the FCs as the unknown. Instead of doing this exercise for each tephra horizon separately, we included all reliably (both isotopic and astronomical) dated tephra to prevent an a priori bias to one of the astronomically dated tephra. However, the calibrated age is an inverse-variance weighted mean age; thus, tephra mes4, with the highest number of replicate analyses and the most precise data, dominates the final outcome. We include only the single-crystal fusion data (displayed here with 1σ analytical error), and ages with P > 0.1. Incremental heating experiments on selected sanidine fractions confirm the thermally undisturbed nature of the samples [14]. We calculate an astronomically calibrated FCs age for each experiment propagating only analytical uncertainties. The weighted mean FCs age and standard analytical error for BGC and VU data are displayed separately and as a combined-age probability diagram. The 28.201 ± 0.012 Ma age for FCs is converted to an intercalibration factor of R^{FCs}_{astro} of 4.3644 ± 0.0018 for a T_{astro} at 6.500 Ma. This translates to 28.201 ± 0.046 Ma, including decay-constant uncertainties and the uncertainty in the astronomical ages of ±10 ky.

Combined 28.201 ± 0.012 Ma
MSWD 0.78; prob 1.00; n=346

VU 28.225 ± 0.019 Ma
MSWD 0.77; prob 0.99; n=189

BGC 28.184 ± 0.016 Ma
MSWD 0.74; prob 0.99; n=157

BGC: ◆ —   VU: ◆ —   Combined: —

Fig. 3. Photo of the upper part of the Zumaia section below the San Telmo chapel. Both the 100-ky limestone beds 29 to 42 of [33] and the large-scale clusters of precession-related basic cycles that mark successive 405-ky eccentricity maxima are indicated (see also figs. S3, a to c). The phase relation with eccentricity is unambiguous: The marly intervals in between the 405- and 100-ky limestone beds often reveal distinct precession-related cycles, which is consistent with eccentricity maxima because eccentricity determines precessional amplitude. Eccentricity minima are marked by weakly developed precession-related cycles and are dominated by limestone beds.

cause eccentricity modulates the precession signal's amplitude.

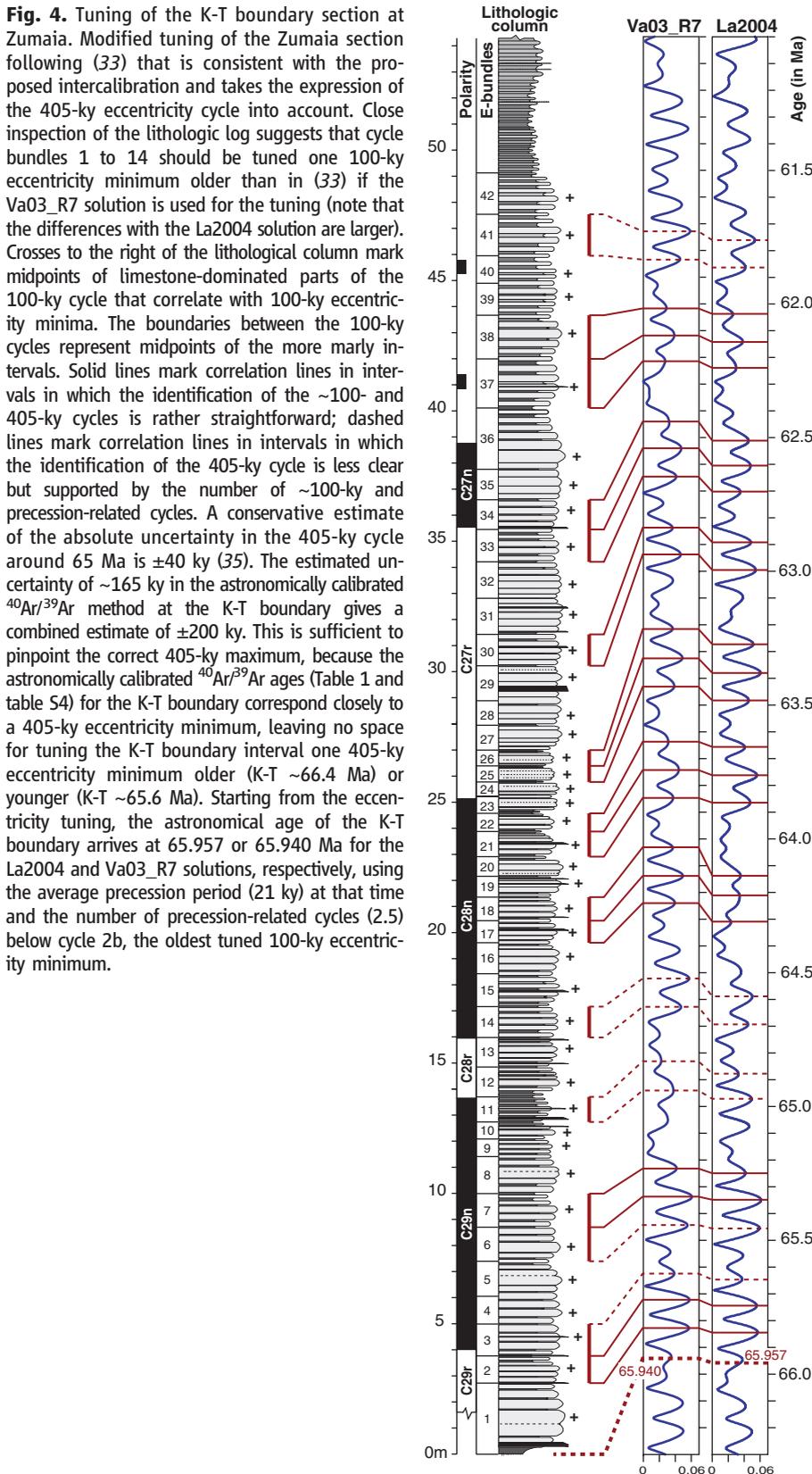The K-T boundary at Zumaia lies at the base of a prominent limestone-dominated interval that corresponds to a 405-ky eccentricity minimum. Successive 405-ky minima have ages of ~65.2, ~65.6, ~66.0, and ~66.4 Ma; thus, the challenge is to identify the correlative minimum. The error in

Fig. 4. Tuning of the K-T boundary section at Zumaia. Modified tuning of the Zumaia section following (33) that is consistent with the proposed intercalibration and takes the expression of the 405-ky eccentricity cycle into account. Close inspection of the lithologic log suggests that cycle bundles 1 to 14 should be tuned one 100-ky eccentricity minimum older than in (33) if the Va03_R7 solution is used for the tuning (note that the differences with the La2004 solution are larger). Crosses to the right of the lithological column mark midpoints of limestone-dominated parts of the 100-ky cycle that correlate with 100-ky eccentricity minima. The boundaries between the 100-ky cycles represent midpoints of the more marly intervals. Solid lines mark correlation lines in intervals in which the identification of the ~100- and 405-ky cycles is rather straightforward; dashed lines mark correlation lines in intervals in which the identification of the 405-ky cycle is less clear but supported by the number of ~100-ky and precession-related cycles. A conservative estimate of the absolute uncertainty in the 405-ky cycle around 65 Ma is ±40 ky (35). The estimated uncertainty of ~165 ky in the astronomically calibrated ^{40}Ar/^{39}Ar method at the K-T boundary gives a combined estimate of ±200 ky. This is sufficient to pinpoint the correct 405-ky maximum, because the astronomically calibrated ^{40}Ar/^{39}Ar ages (Table 1 and table S4) for the K-T boundary correspond closely to a 405-ky eccentricity minimum, leaving no space for tuning the K-T boundary interval one 405-ky eccentricity minimum older (K-T ~66.4 Ma) or younger (K-T ~65.6 Ma). Starting from the eccentricity tuning, the astronomical age of the K-T boundary arrives at 65.957 or 65.940 Ma for the La2004 and Va03_R7 solutions, respectively, using the average precession period (21 ky) at that time and the number of precession-related cycles (2.5) below cycle 2b, the oldest tuned 100-ky eccentricity minimum.

the astronomical solution is on the order of 40 ky at 65 Ma [(34) and figure 25 in (35)]. To pinpoint this minimum, we recalculated published ^{40}Ar/^{39}Ar ages for the K-T boundary interval with our astronomical FCs age of 28.201 Ma.

Single-crystal sanidine ^{40}Ar/^{39}Ar dates on tephra horizons are available for the same magnetostratigraphic interval in continental sections in Montana (36). Haïtian K-T boundary tektites and Chixulub crater melt rock have also been dated by the ^{40}Ar/^{39}Ar technique (37, 38). These ages recalculated relative to our FCs age of 28.201 Ma range from 65.8 to 66.0 Ma (Table 1 and table S4). We regard the single-crystal sanidine ages of 65.84 Ma [of Z coal (36)] and especially 65.99 Ma [of IrZ coal (36)] as the best estimates. These ages are considerably greater than the ages reported in GTS2004, which are based on sea-floor anomaly profiles numerically calibrated by means of a limited number of isotopically dated tie points, including the K-T boundary at 65.5 Ma, using an age of 28.02 Ma for FCs. This approach pins the K-T boundary down to the 405-ky eccentricity minimum around 66.0 Ma. Using this calibration as the starting point, the Zumaia section of (33) was retuned, taking the newly recognized 405-ky cycle into account (Figs. 3, 4). The resultant astronomical ages for the K-T boundary and magnetic reversal boundaries are in good agreement with the revised ^{40}Ar/^{39}Ar ages (Table 1).

In principle, the revised astronomical age of ~65.95 Ma for the K-T boundary can be shifted upward or downward by one 405-ky eccentricity cycle, resulting in ages of either ~65.56 or ~66.4 Ma (for example, see fig. S4). However, the astronomically recalibrated ^{40}Ar/^{39}Ar ages allow us to exclude these ages for the K-T boundary (Table 1 and table S4). Westerhold et al. (39) similarly linked the K-T boundary to a 405-ky eccentricity minimum using Fe and magnetic susceptibility records of Ocean Drilling Program cores from the Pacific and Atlantic Ocean and including the Zumaia section in their astrochronological framework. Their preferred tuning options result in ages of 65.28 Ma (option 1) or 65.68 Ma (option 2) for the K-T boundary. A third option (66.08 Ma) was added for consistency with our astronomically calibrated age for FCs, but this option is less favored, because it results in a relatively old age of 56.33 Ma for the Paleocene/Eocene boundary, an age that is difficult to reconcile with existing, though limited, radioisotopic constraints, even when recalculated against our astronomical FCs age. However, our Zumaia tuning results in one extra 405-ky cycle compared with (39) for the interval between the K-T boundary and the top of the normal polarity interval of C28n. Such differences must be resolved before a tuned Paleocene time scale can be finalized. Nevertheless, our intercalibration firmly links the K-T boundary to the 405-ky eccentricity minimum around 66 Ma.

An age of ~66.0 Ma for the K-T boundary was previously incorporated in the polarity time scale of Cande and Kent (40). However, this seemingly identical age was interpreted to be a spurious result from the chemical preparation of volcanic ashes

found intercalated in coal beds. Redating of the sanidine in these ash beds (using an age of 27.83 Ma for the FCs) led to a revised age of ~ 65.0 Ma for the K-T boundary, which was adopted in (*41*). The same single-crystal sanidine dates now provide an age of ~ 65.95 Ma, relative to our FCs age of 28.201 Ma.

We argue that our astronomically calibrated FCs age of 28.201 Ma should be incorporated in the next standard GTS to recalculate all other $^{40}Ar/^{39}Ar$ ages after it is confirmed by independent (intercalibration) studies. Only in this way is a mutually consistent age calibration of the GTS assured. Moreover, our integrated approach may lead to a stable time scale with unprecedented accuracy, precision, and resolution that will not be forced to undergo any further substantial revisions.

References and notes

1. F. M. Gradstein, J. G. Ogg, A. G. Smith, *A Geologic Time Scale 2004* (Cambridge Univ. Press, Cambridge, 2004).
2. P. R. Renne, D. B. Karner, K. R. Ludwig, *Science* **282**, 1840 (1998).
3. K. F. Kuiper, F. J. Hilgen, J. Steenbrink, J. R. Wijbrans, *Earth Planet. Sci. Lett.* **222**, 583 (2004).
4. P. R. Renne *et al.*, *Chem. Geol.* **145**, 117 (1998).
5. K. W. Min, R. Mundil, P. R. Renne, K. R. Ludwig, *Geochim. Cosmochim. Acta* **64**, 73 (2000).
6. All errors are stated at the 2σ level, unless stated otherwise.
7. P. R. Renne *et al.*, *Geology* **22**, 783 (1994).
8. F. J. Hilgen, W. Krijgsman, J. R. Wijbrans, *Geophys. Res. Lett.* **24**, 2043 (1997).
9. J. Steenbrink, N. Van Vugt, F. J. Hilgen, J. R. Wijbrans, J. E. Meulenkamp, *Palaeogeogr. Palaeoclimatol. Palaeoecol.* **152**, 283 (1999).
10. S. Roger *et al.*, *Earth Planet. Sci. Lett.* **179**, 101 (2000).
11. E. Van Assen, K. F. Kuiper, N. Barhoun, W. Krijgsman, F. J. Sierro, *Palaeogeogr. Palaeoclimatol. Palaeoecol.* **238**, 15 (2006).
12. W. Krijgsman, F. J. Hilgen, I. Raffi, F. J. Sierro, D. S. Wilson, *Nature* **400**, 652 (1999).
13. L. J. Lourens, F. J. Hilgen, J. Laskar, N. J. Shackleton, D. Wilson, in *The Geological Time Scale 2004*, F. M. Gradstein, J. G. Ogg, A. G. Smith, Eds. (Cambridge Univ. Press, Cambridge, 2004), pp. 409–440.
14. Materials and methods are available as supporting material on *Science* Online.
15. R. H. Steiger, E. Jäger, *Earth Planet. Sci. Lett.* **36**, 359 (1977).
16. J. I. Simon, P. R. Renne, R. Mundil, *Earth Planet. Sci. Lett.* **266**, 182 (2008).
17. O. Bachmann *et al.*, *Chem. Geol.* **236**, 134 (2007).
18. M. D. Schmitz, S. A. Bowring, *Geochim. Cosmochim. Acta* **65**, 2571 (2001).
19. B. Schoene, J. L. Crowley, D. J. Condon, M. D. Schmitz, S. A. Bowring, *Geochim. Cosmochim. Acta* **70**, 426 (2006).
20. R. Mundil, P. R. Renne, K. K. Min, K. R. Ludwig, *Eos Transactions American Geophysical Union Meeting Supplement* **87**, Abstract V21A (2006).
21. J. Y. Kwon, K. W. Min, P. J. Bickel, P. R. Renne, *Math. Geol.* **34**, 457 (2002).
22. Acapulco has chondritic chemistry but lacks chondrules owing to early high-temperature metamorphism (*42*).
23. P. R. Renne, *Earth Planet. Sci. Lett.* **175**, 13 (2000).
24. E. K. Jessberger, B. Dominik, T. Staudacher, G. F. Herzog, *Icarus* **42**, 380 (1980).
25. Y. Amelin, V. Pravdivtseva, *Meteorit. Planet. Sci.* **40**, A16 (2005).
26. A. Bouvier, J. Blichert-Toft, F. Moynier, J. D. Vervoort, F. Albarede, *Geochim. Cosmochim. Acta* **71**, 1583 (2007).
27. K. Min, K. A. Farley, P. R. Renne, K. Marti, *Earth Planet. Sci. Lett.* **209**, 323 (2003).
28. R. H. Nichols, C. M. Hohenberg, K. Kehm, Y. Kim, K. Marti, *Geochim. Cosmochim. Acta* **58**, 2553 (1994).
29. T. D. Swindle, *Meteorit. Planet. Sci.* **33**, 1147 (1998).
30. R. S. Coe, B. S. Singer, M. S. Pringle, X. X. Zhao, *Earth Planet. Sci. Lett.* **222**, 667 (2004).
31. L. J. Lourens *et al.*, *Nature* **435**, 1083 (2005).
32. H. Pälike *et al.*, *Science* **314**, 1894 (2006).
33. J. Dinarès-Turell *et al.*, *Earth Planet. Sci. Lett.* **216**, 483 (2003).
34. H. Pälike, J. Laskar, N. J. Shackleton, *Geology* **32**, 929 (2004).
35. J. Laskar *et al.*, *Astron. Astrophys.* **428**, 261 (2004).
36. C. C. Swisher, L. Dingus, R. F. Butler, *Can. J. Earth Sci.* **30**, 1981 (1993).
37. C. C. Swisher III *et al.*, *Science* **257**, 954 (1992).
38. G. A. Izett, G. B. Dalrymple, L. W. Snee, *Science* **252**, 1539 (1991).
39. T. Westerhold *et al.*, *Palaeogeogr. Palaeoclimatol. Palaeoecol.* **257**, 377 (2008).
40. S. C. Cande, D. V. Kent, *J. Geophys. Res.* **97**, 13917 (1992).
41. W. A. Berggren, D. V. Kent, C. C. Swisher, M.-P. Aubry, *Geochronology, Time Scales and Global Stratigraphic Correlation, SEPM Special Publication* **54**, 129 (1995).
42. T. J. McCoy *et al.*, *Geochim. Cosmochim. Acta* **60**, 2681 (1996).
43. F. J. Sierro, F. J. Hilgen, W. Krijgsman, J. A. Flores, *Palaeogeogr. Palaeoclimatol. Palaeoecol.* **168**, 141 (2001).
44. F. Varadi, B. Runnegar, M. Ghil, *Astrophys. J.* **592**, 620 (2003).
45. The project was funded by grants 750.198.02 and 814.01.004 of the Netherlands Organisation for Scientific Research to K.K., and supported by NSF grant EAR-9903078 to P.R. and A.D. P.R. and A.D.'s work was also supported by the Ann and Gordon Getty Foundation. Mineral separation facilities at VU were provided by Roel van Elsas.

REPORTS

Sign Change of Poisson's Ratio for Carbon Nanotube Sheets

Lee J. Hall,[1] Vitor R. Coluci,[2] Douglas S. Galvão,[2] Mikhail E. Kozlov,[1] Mei Zhang,[1]* Sócrates O. Dantas,[3] Ray H. Baughman[1]†

Most materials shrink laterally like a rubber band when stretched, so their Poisson's ratios are positive. Likewise, most materials contract in all directions when hydrostatically compressed and decrease density when stretched, so they have positive linear compressibilities. We found that the in-plane Poisson's ratio of carbon nanotube sheets (buckypaper) can be tuned from positive to negative by mixing single-walled and multiwalled nanotubes. Density-normalized sheet toughness, strength, and modulus were substantially increased by this mixing. A simple model predicts the sign and magnitude of Poisson's ratio for buckypaper from the relative ease of nanofiber bending and stretch, and explains why the Poisson's ratios of ordinary writing paper are positive and much larger. Theory also explains why the negative in-plane Poisson's ratio is associated with a large positive Poisson's ratio for the sheet thickness, and predicts that hydrostatic compression can produce biaxial sheet expansion. This tunability of Poisson's ratio can be exploited in the design of sheet-derived composites, artificial muscles, gaskets, and chemical and mechanical sensors.

When stretched, most materials contract in both lateral dimensions to decrease stretch-induced volume change. The ratio of percent lateral contraction to percent applied tensile elongation is the Poisson's ratio. Some rubbers have Poisson's ratios of about 0.5 for both lateral directions, so their volume does not appreciably change upon stretching. In very rare materials the sum of Poisson's ratios for lateral dimension changes exceeds unity, so they increase density when stretched and, inversely, expand in at least one direction when hydrostatically compressed (*1*). If a lateral dimension expands during stretching, the associated Poisson's ratio is negative and the material is called auxetic (*2*). Recent interest in this counterintuitive behavior originated from pioneering discoveries that partially collapsed foams and honeycombs (*2, 3*), fibrillar polymers (*4*), and polymer composites (*5*) can be auxetic.

Poisson's ratio was unknowingly used 2000 years ago in the empirical selection of cork for wine bottle stoppers. Cork stoppers have a near-zero Poisson's ratio for radial directions when subjected to orthogonal uniaxial stress (*6*). A positive Poisson's ratio makes a stopper difficult to insert but easy to remove, and the reverse occurs for a negative Poisson's ratio.

Carbon nanotube sheets (buckypaper) were fabricated (*7, 8*) by filtration of aqueous dispersions of single-walled nanotubes (SWNTs) (*9*) and multiwalled carbon nanotubes (MWNTs) (*10*) produced by chemical vapor deposition, a technique reminiscent of ancient methods for making writing paper by drying a fiber slurry. The SWNTs are seamless cylinders of graphite